

**Figure S1.** Schematic diagram of the dry extraction system used for this study. Details are described in Ahn et al. (2009). He-CCR stands for He-Closed Cycled Refrigerator.

**Table S1.** Comparison of CO<sub>2</sub> analysis with two different standard airs (188.9 and 293.3 ppm) in order to check the linearity in the gas chromatograph.

| Siple<br>Dome<br>ice core | With 188.9 ppm Standard air |                                  |                      |                 | With 293.3 ppm Standard air |                                  |                      |                 | Difference               |                      |
|---------------------------|-----------------------------|----------------------------------|----------------------|-----------------|-----------------------------|----------------------------------|----------------------|-----------------|--------------------------|----------------------|
| Mean<br>depth<br>(m)      | CO <sub>2</sub><br>(ppm)    | mean<br>CO <sub>2</sub><br>(ppm) | uncertainty<br>(ppm) | # of<br>samples | CO <sub>2</sub><br>(ppm)    | mean<br>CO <sub>2</sub><br>(ppm) | uncertainty<br>(ppm) | # of<br>samples | CO <sub>2</sub><br>(ppm) | uncertainty<br>(ppm) |
| 640.53                    | 248.7                       | 249.6                            | 0.9                  | 2               | 250.7                       | 249.6                            | 0.9                  | 3               | 0.0                      | 1.3                  |
|                           | 250.5                       |                                  |                      |                 | 247.8                       |                                  |                      |                 |                          |                      |
| 644.22                    | 246.0                       | 246.0                            | 0.1                  | 2               | 247.8                       | 247.2                            | 0.6                  | 2               | 1.2                      | 0.6                  |
|                           | 246.1                       |                                  |                      |                 | 246.6                       |                                  |                      |                 |                          |                      |
| 668.09                    | 241.7                       | 242.2                            | 0.5                  | 2               | 242.3                       | 243.1                            | 0.8                  | 2               | 0.9                      | 0.9                  |
|                           | 242.7                       |                                  |                      |                 | 243.8                       |                                  |                      |                 |                          |                      |
| 671.51                    | 243.7                       | 243.0                            | 0.7                  | 2               | 242.8                       | 243.5                            | 0.4                  | 3               | 0.5                      | 0.8                  |
|                           | 242.3                       |                                  |                      |                 | 243.5                       |                                  |                      |                 |                          |                      |
| 673.47                    | 241.1                       | 240.4                            | 0.8                  | 2               | 244.2                       |                                  |                      |                 |                          |                      |
|                           | 239.6                       |                                  |                      |                 | 239.1                       | 239.8                            | 0.7                  | 2               | -0.6                     | 1.0                  |
|                           |                             |                                  |                      |                 | 240.5                       |                                  |                      |                 |                          |                      |
| Average                   |                             |                                  |                      |                 |                             |                                  |                      |                 | 0.4                      | 0.9                  |

**Table S2.** Interlaboratory comparison between SNU (Seoul National University) and OSU (Oregon State University) using Siple Dome ice core.

| Depth range        | SNU CO <sub>2</sub> | # of replicates | OSU CO <sub>2</sub> | #of replicates | SNU-OSU |
|--------------------|---------------------|-----------------|---------------------|----------------|---------|
| (m)                | (ppm)               |                 | (ppm)               |                | (ppm)   |
| 490.17–490.22      | 266.8               | 2               | 265.7               | 3              | 1.1     |
| 500.40–500.45      | 263.8               | 2               | 264.1               | 4              | -0.3    |
| 501.87–502.41      | 263.8               | 2               | 262.8               | 2              | 1.1     |
| 506.60–506.65      | 264.9               | 3               | 265.0               | 2              | -0.1    |
| 522.90–523.10      | 266.7               | 2               | 266.3               | 2              | 0.5     |
| 523.28–523.33      | 265.2               | 2               | 265.8               | 2              | -0.6    |
| 530.50–530.55      | 266.9               | 2               | 266.4               | 2              | 0.6     |
| Average            |                     |                 |                     |                | 0.3     |
| Standard deviation |                     |                 |                     |                | 0.7     |

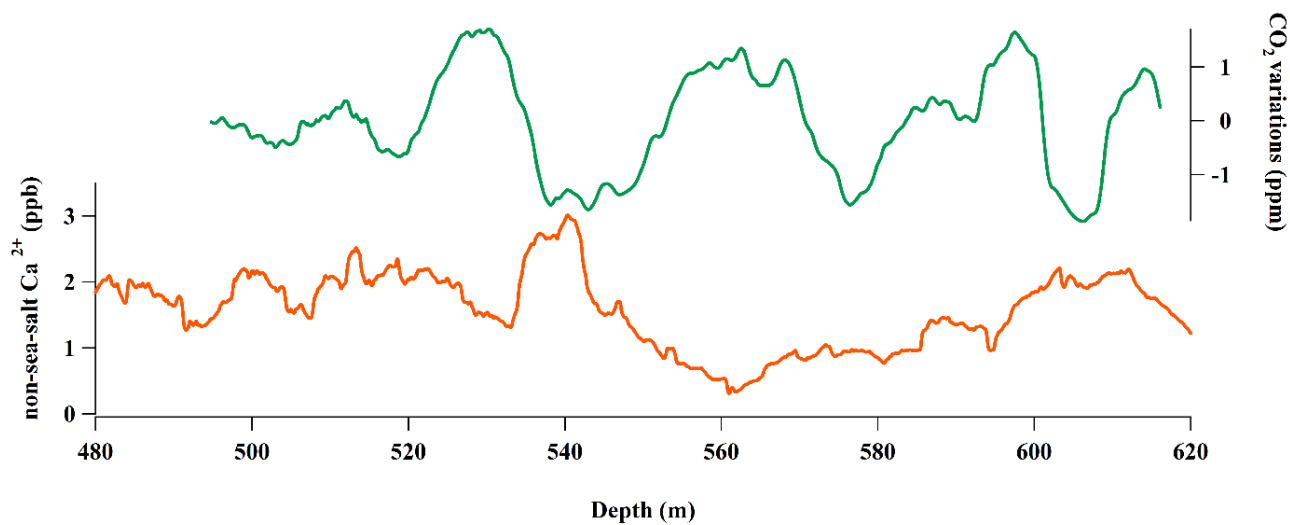


**Figure S2.** Comparison of Siple Dome millennial (filtered) CO<sub>2</sub> record (Ahn et al., 2014) and non-sea-salt Ca<sup>2+</sup> on depth domain. The non-sea-salt Ca<sup>2+</sup> data are 250-yr running means.

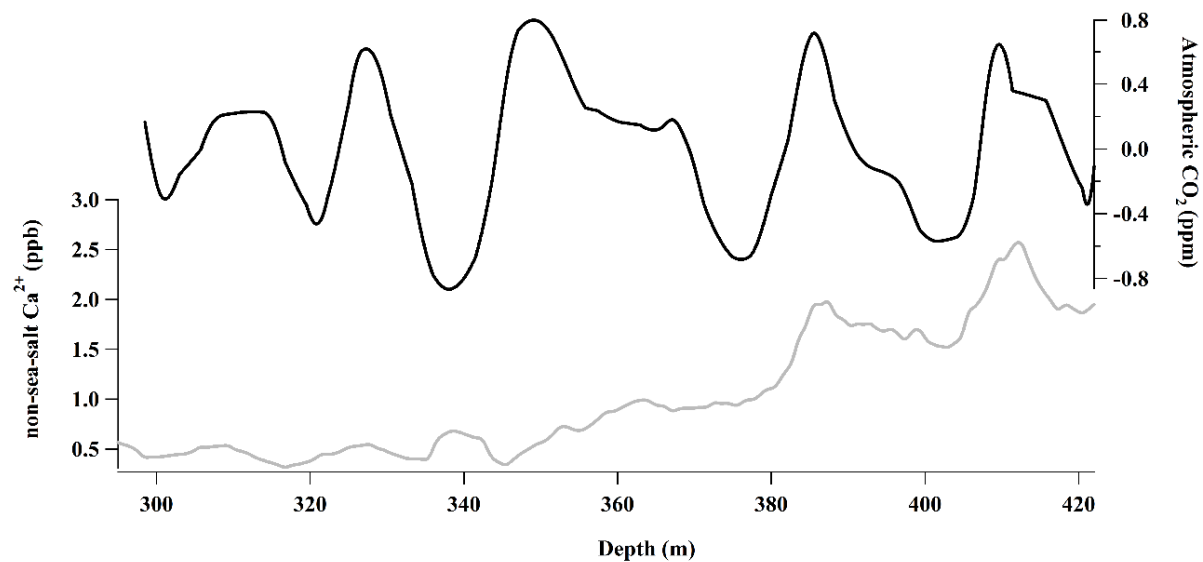


**Figure S3.** Comparison of Dome C millennial (filtered)  $\text{CO}_2$  record (Monnin et al., 2001; Monnin et al., 2004) and non-sea-salt  $\text{Ca}^{2+}$  (Lambert et al., 2012) on depth domain. The non-sea-salt  $\text{Ca}^{2+}$  data are 250-yr running means.

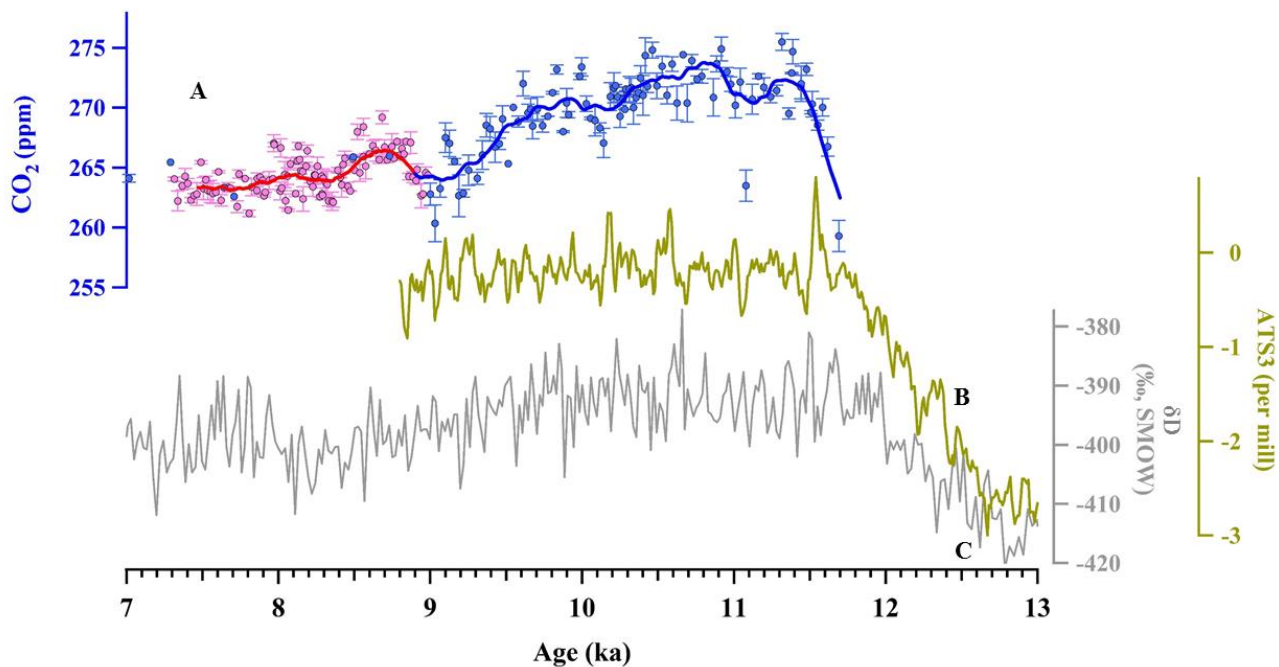


**Figure S4.** High-resolution atmospheric CO<sub>2</sub> records obtained from Siple Dome ice core, Antarctica during the early Holocene.

A) Pink and blue circles are Siple Dome ice core records obtained at OSU (Ahn et al., 2014) and SNU (this study), respectively.

- 5 Lines in pink and blue represent 250-yr running means. B) Antarctic temperature Stack 3 (ATS3) developed by Buizert et al. (2018) using five records: Dome C, Dome Fuji, Talos Dome, EPICA Dronning Maud Land and WAIS Divide. C) Grey line indicates δD in the Dome C ice core, Antarctica (Jouzel et al., 2007).

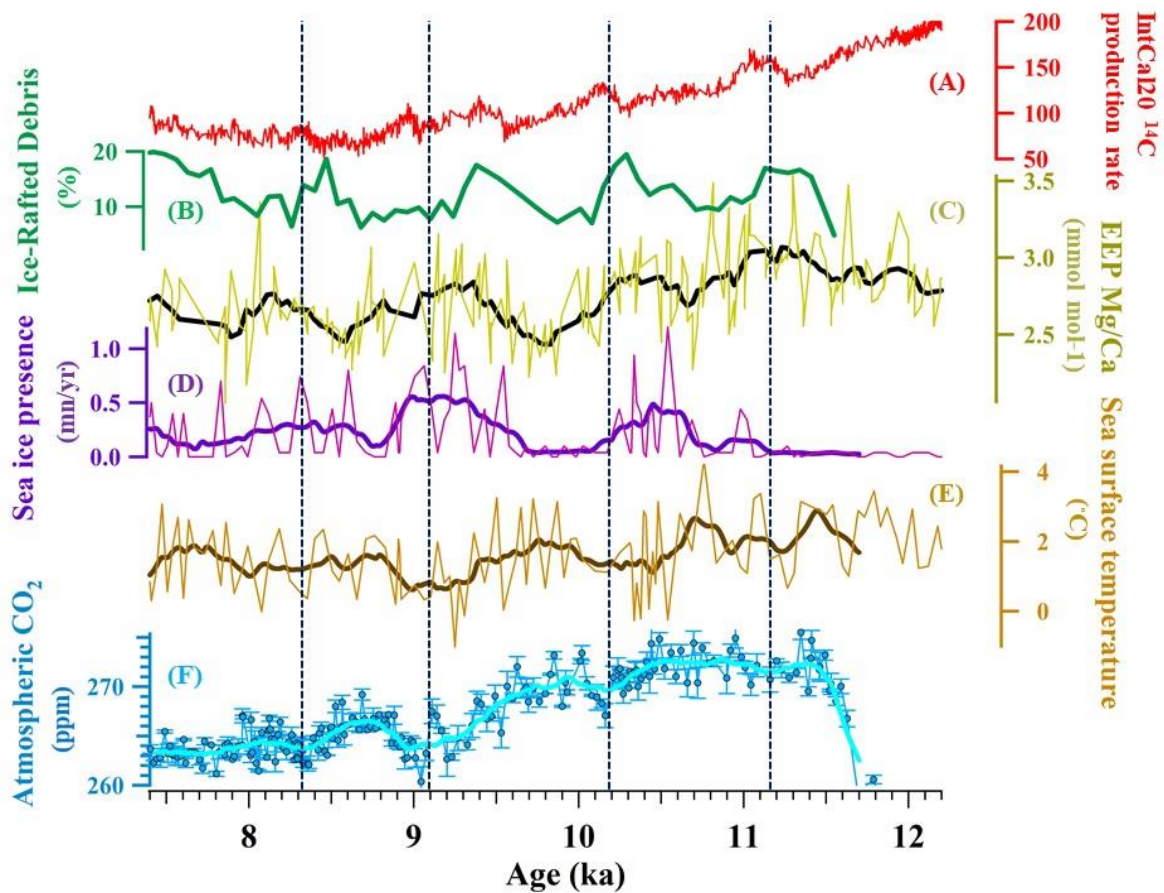


**Figure S5.** Comparison of atmospheric CO<sub>2</sub> with climatic proxy records over the early Holocene. Lines represent 250-yr running means. (A) IntCal20<sup>14</sup>C production rate (Reimer et al., 2020). (B) Ice rafted debris stacked records from the North Atlantic regions on untuned calibrated <sup>14</sup>C age model (Bond et al., 2001; Marchitto et al., 2010). (C) Sea surface temperature from the eastern equatorial Pacific indicating El Niño-like or La Niña-like conditions (Marchitto et al., 2010). (D) Sea ice presence from the Polar Front of the Southern Ocean on the chronology of Mortyn et al. (2003) (Nielsen et al., 2004). (E) Sea surface temperature from the Polar Front of the Southern Ocean on the chronology of Mortyn et al. (2003) (Nielsen et al., 2004). (F) Atmospheric CO<sub>2</sub> record from Siple Dome (in this study).

## Monte Carlo simulation

We calculate uncertainties of a smoothed CO<sub>2</sub> record by using Monte Carlo simulation (Figure 1). Random sampling was made from a probability distribution for each measured value and its standard deviation. We repeated this series of simulations 10,000 times, which is shown as 2 $\sigma$  in Figure 1

- 5 The uncertainty band is narrow, which is attributed to the removal of the high frequency signal by 250-yr running means. When the Monte Carlo simulation was conducted, we considered that each data follows a normal distribution. The width of the error band is affected by neighbouring data points. If the data points are close together, the error of neighbouring data points in the opposite direction can be canceled out, resulting in a narrow uncertainty band.

We evaluated 250-yr running means and their uncertainties by using a new Monte Carlo approach. Random sampling was made from a probability distribution for each measured value and its standard deviation. If the standard deviation was smaller than the average reproducibility of the measurement ( $1\sigma = 0.87$  ppm), we used 0.87 ppm as the uncertainty of a measured value. Then, 1-yr interpolation and resampling were applied to generate an evenly-spaced time series and to calculate the 250-yr running means. We repeated this series of simulations 10,000 times and evaluated the mean of 250-yr running means and its uncertainty (shown as 2 $\sigma$  in Figure S6). We used a modified Akima method using the built-in makima function in Matlab

10  
15 for the interpolation. The different types of interpolation and smoothing methods resulted in insignificant differences in the 250-yr running means.

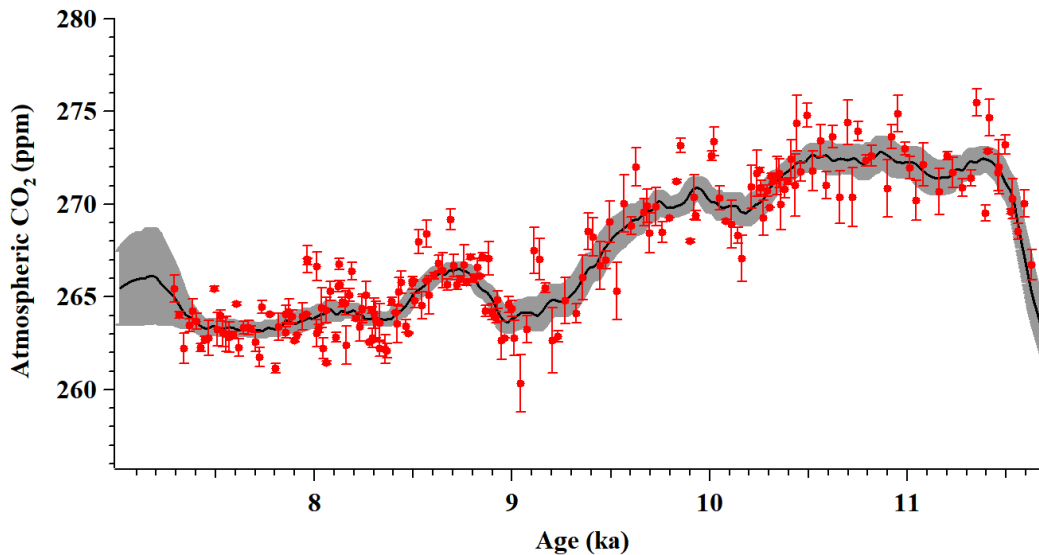


**Figure S6.** Red circles are Siple Dome ice core records during the early Holocene (11.7–7.4 ka). The black line indicates the average of 10,000 times modified akima simulations showing an error-weighted average of the CO<sub>2</sub> record. The dark shaded indicates 2 $\sigma$  uncertainties calculated from modified akima simulations.



## Correlation coefficients between CO<sub>2</sub> and climate proxies

In order to assess the relationship between CO<sub>2</sub> and climate, we calculate correlations and estimate leads and lags between CO<sub>2</sub> and proxies of solar activity as well as climate proxies thought to be themselves related to solar activity. The Pearson correlation coefficient  $r$  is commonly used to verify relationships between variables. However,  $r$  does not take chronological uncertainty into account. As such, we apply a Monte Carlo procedure to estimate the correlations between CO<sub>2</sub> and climate proxies. In the procedure, we adjust the chronologies of the two series, within their chronological uncertainties, and re-calculate  $r$ . We do so 1,000 times for each pair, allowing us to calculate a mean correlation coefficient that is more representative of the relationship between time-uncertain series.

We use a similar method to calculate the significance of this correlation against a random red-noise process. At each of the 1,000 steps, we use an AR(1) model (lag-1 auto regression) to fit data series. We then use these AR(1) characteristics to randomly generate two synthetic series with the same red noise. Then, we calculate the percentage of correlations between the randomized synthetic series that are lower than the correlation coefficients of the real series to assess the significance of the correlation.

Finally, we can calculate the maximum-correlation lag between the two series. At each step in the 1,000 iteration Monte Carlo procedure, we calculate the lag which gives the maximum correlation by shifting one of the series by 10-yr increments, for constant lags between -200 (a CO<sub>2</sub> lead) and 200 yrs (a CO<sub>2</sub> lag). Then, we make a histogram of the calculated maximum-correlation lags, from which the mode can be selected as an approximation of the phasing between the two series. We also report the maximum correlation between the two series, but note that this is not representative of the actual relationship (it simply gives an idea of how much the correlation can be improved by adding a lag between the two series).

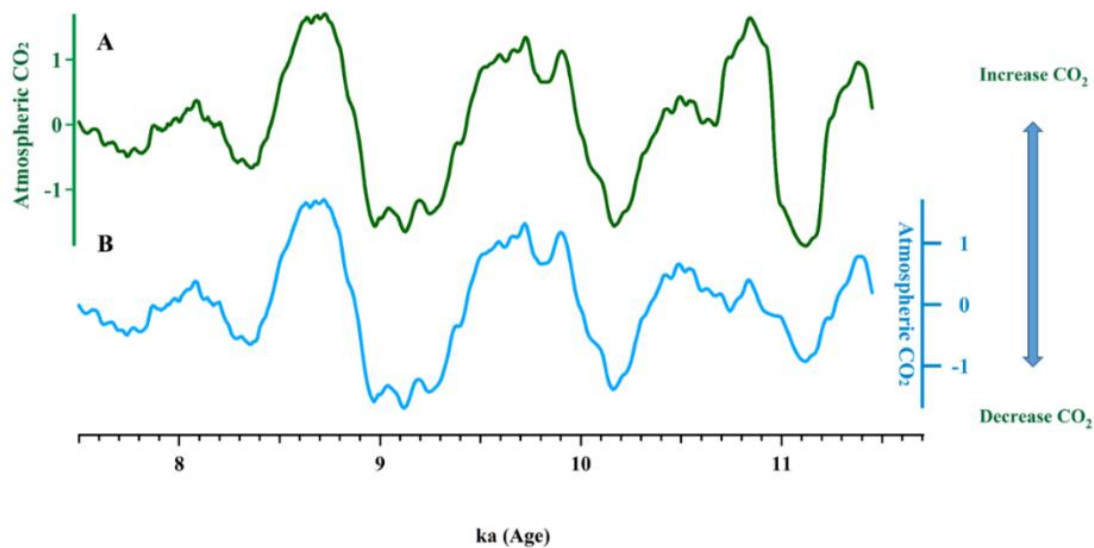


**Figure S7.** (A) Green line indicates CO<sub>2</sub> original data which was filtered by high pass filtering. (B) Blue line indicates CO<sub>2</sub> data filtered by high pass filtering without 2 points at 11.8 ka and 10.825 ka.

**Table S3.** Correlation between Siple Dome CO<sub>2</sub> record without single outliers at 10.8 ka and 11.1 ka and climate proxy records. Column A shows correlation coefficients between CO<sub>2</sub> and proxies with CO<sub>2</sub> time lags. Column B shows correlation coefficients between CO<sub>2</sub> and proxies without CO<sub>2</sub> time lag. “With MC” are mean values from the simulations taking age uncertainties into account. “Without MC” is the classic calculation of correlation, without taking age uncertainty into account.

5 Significance of the lag correlations was assessed against 1,000 repetitions of the lag correlation calculation using synthetic data stochastically generated to have the same red noise characteristics as the original series.

| Proxy records   | A: Correlation between CO <sub>2</sub> and proxies with CO <sub>2</sub> time lag (yrs) |                  |                   |          | B: Correlation between CO <sub>2</sub> and proxies without CO <sub>2</sub> time lag |                   |
|---|--|------------------|-------------------|----------|---|-------------------|
|   | With MC  |                  | Without MC        |          | With MC   | Without MC        |
|   | r (p-value)  | Time lag         | r (p-value)       | Time lag | r (p-value)   | r (p-value)       |
| CO <sub>2</sub> - <sup>14</sup> C production rate<br>Marchitto et al.(2010);<br>Reimer et al.(2004)   | -0.44±0.10<br>(0.010)  | 0±148            | -0.76<br>(<0.001) | 40       | -0.43<br>(0.005)  | -0.62<br>(<0.001) |
| CO <sub>2</sub> - <sup>10</sup> Be flux from Greenland ice core<br>Finkel and Nishiizumi (1997);<br>Marchitto et al. (2010);<br>Vonmoos et al. (2006) | -0.30±0.06<br>(0.101)  | 130±63           | -0.58<br>(<0.001) | 120      | -0.30<br>(0.021)  | -0.36<br>(<0.001) |
| CO <sub>2</sub> - IRD from the North Atlantic region<br>Bond et al. (2001);<br>Marchitto et al. (2010)  | -0.44±0.11<br>(0.076)  | 70±155           | -0.73<br>(<0.001) | 160      | -0.32<br>(0.057)  | -0.23<br>(0.001)  |
| CO <sub>2</sub> - SST from eastern equatorial Pacific<br>Marchitto et al. (2010)  | -0.37±0.13<br>(0.057)  | 0±219            | -0.61<br>(<0.001) | 80       | -0.34<br>(0.044)  | -0.56<br>(<0.001) |
| CO <sub>2</sub> - Sea ice in the Southern Ocean<br>Nielsen et al. (2004)  | -0.32±0.16<br>(0.171)  | -<br>180±22<br>8 | -0.57<br>(<0.001) | 80       | -0.24<br>(0.155)  | -0.49<br>(<0.001) |
| CO <sub>2</sub> - SST in the Southern Ocean<br>Nielsen et al. (2004)  | 0.35±0.16<br>(0.075)   | 60±228           | 0.58<br>(<0.001)  | 20       | 0.35<br>(0.063)   | 0.58<br>(<0.001)  |
| CO <sub>2</sub> - NGRIP δ <sup>18</sup> O<br>Rasmussen et al. (2006)  | 0.18±0.06<br>(0.180)   | -<br>140±63      | 0.20<br>(0.080)   | -110     | 0.17<br>(0.180)   | 0.16<br>(0.001)   |

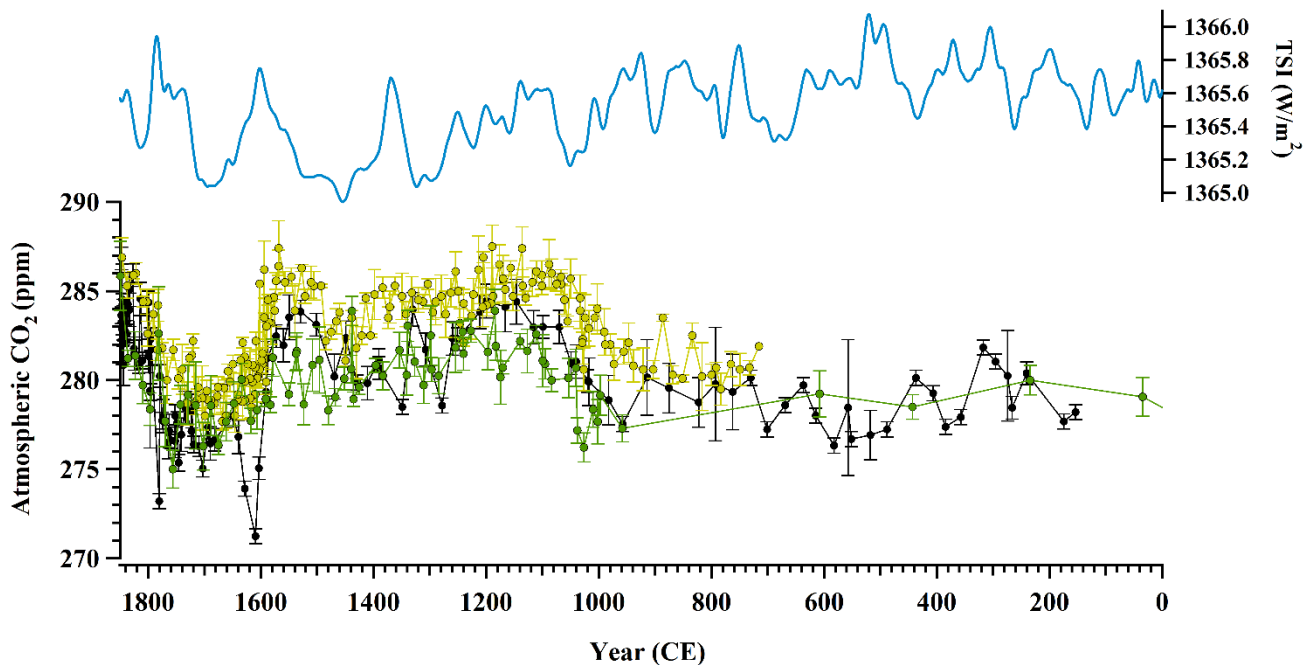


**Figure S8.** Atmospheric CO<sub>2</sub> from Antarctic ice cores during the last 2,000 yrs. Blue line: total solar irradiance (TSI) (Roth and Joos, 2013). Yellow dots: atmospheric CO<sub>2</sub> from WAIS Divide ice core (Ahn et al., 2012). Green dots: atmospheric CO<sub>2</sub> from EPICA Dronning Maud Land (EDML) (Monnin et al., 2004; Siegenthaler et al., 2005). Black dots: atmospheric CO<sub>2</sub> from Law Dome (Rubino et al., 2019).

## References

- Ahn, J., Brook, E. J., and Buizert, C.: Response of atmospheric CO<sub>2</sub> to the abrupt cooling event 8200 years ago, *Geophys. Res. Lett.*, 41, 604–609, <https://doi.org/10.1002/2013gl058177>, 2014.
- Ahn, J., Brook, E. J., Mitchell, L., Rosen, J., McConnell, J. R., Taylor, K., Etheridge, D., and Rubino, M.: Atmospheric CO<sub>2</sub> over the last 1000 years: A high-resolution record from the West Antarctic Ice Sheet (WAIS) Divide ice core, *Global Biogeochem. Cy.*, 26, GB2027, <https://doi.org/10.1029/2011GB004247>, 2012.
- Ahn, J. H., Brook, E. J., and Howell, K.: A high-precision method for measurement of paleoatmospheric CO<sub>2</sub> in small polar ice samples, *J. Glaciol.*, 55, 499–506, 2009.
- Bond, G., Kromer, B., Beer, J., Muscheler, R., Evans, M. N., Showers, W., Hoffmann, S., Lotti-Bond, R., Hajdas, I., and Bonani, G.: Persistent solar influence on North Atlantic climate during the Holocene, *Science*, 294, 2130–2136, 2001.
- Buizert, C., Sigl, M., Severi, M., Markle, B. R., Wettstein, J. J., McConnell, J. R., Pedro, J. B., Sodemann, H., Goto-Azuma, K., Kawamura, K., et al.: Abrupt ice-age shifts in southern westerly winds and Antarctic climate forced from the north, *Nature*, 563, 681–685, 2018.
- Finkel, R. C. and Nishiizumi, K.: Beryllium 10 concentrations in the Greenland Ice Sheet Project 2 ice core from 3–40 ka, *J. Geophys. Res.*, 102(C12), 26699–26706, doi:199710.1029/97JC01282, 1997.
- Jouzel, J., Masson-Delmotte, V., Cattani, O., Dreyfus, G., Falourd, S., Hoffmann, G., Minster, B., Nouet, J., Barnola, J. M., Chappellaz, J., Fischer, H., Gallet, J. C., Johnsen, S., Leuenberger, M., Loulergue, L., Luethi, D., Oerter, H., Parrenin, F., Raisbeck, G., Raynaud, D., Schilt, A., Schwander, A., Selmo, E., Souchez, R., Spahni, R., Stauffer, B., Steffensen, J. P., Stenni, B., Stocker, T.F., Tison, J. L., Werner, M., and Wolff, E. W.: Orbital and Millennial Antarctic Climate Variability over the Past 800,000 Years, *Science*, 317, 793–796, <https://doi.org/10.1126/science.1141038>, 2007.
- Lambert, F., Bigler, M., Steffensen, J. P., Hutterli, M., and Fischer, H.: Centennial mineral dust variability in high-resolution ice core data from Dome C, Antarctica, *Clim. Past*, 8, 609–623, <https://doi.org/10.5194/cp-8-609-2012>, 2012.
- Marchitto, T. M., Muscheler, R., Ortiz, J. D., Carriquiry, J. D., and van Geen, A.: Dynamical response of the tropical Pacific Ocean to solar forcing during the early Holocene, *Science*, 330, 1378–1381, 2010.
- Monnin, E., Steig, E. J., Siegenthaler, U., Kawamura, K., Schwander, J., Stauffer, B., Stocker, T. F., Morse, D. C., Barnola, J.-M., Bellier, B., Raynaud, D., and Fischer, H.: Evidence for substantial accumulation rate variability in Antarctica during the Holocene through synchronization of CO<sub>2</sub> in the Taylor Dome, Dome C and DML ice cores, *Earth Planet. Sc. Lett.*, 224, 45–54, 2004.
- Monnin, E., Indermuhle, A., Dallenbach, A., Fluckiger, J., Stauffer, B., Stocker, T. F., Raynaud, D., and Barnola, J.-M.: Atmospheric CO<sub>2</sub> concentrations over the last glacial termination, *Science*, 291(5501), 112–114, 2001.
- Mortyn, P. G., Charles, C. D., Ninnemann, U. S., Ludwig, K., and Hodell, D. A.: Deep sea sedimentary analogues for the Vostok ice core, *Geochem. Geophys. Geosy.*, 4, 8405, doi:10.1029/2002GC000475, 2003.

- Nielsen, S. H. H., Koc, N., and Crosta, X.: Holocene climate in the Atlantic sector of the southern ocean: Controlled by insolation or oceanic circulation?, *Geology*, 32, 317–320, 2004.
- Rasmussen, S. O., Andersen, K. K., Svensson, A. M., Steffensen, J. P., Vinther, B. M., Clausen, H. B., Siggaard-Andersen, M.-L., Johnsen, S. J., Larsen, L. B., Dahl-Jensen, D., Bigler, M., Rothlisberger, R., Fischer, H., Goto-Azuma, K., Hansson, M.E., and Ruth, U.: A new Greenland ice core chronology for the last glacial termination, *J. Geophys. Res.*, 111, D06102, <https://doi.org/10.1029/2005JD006079>, 2006.
- Reimer, P. J., Austin, W. E. N., Bard, E., Bayliss, A., Blackwell, P. G., Ramsey, C. B., Butzin, M., Cheng, H., Edwards, R. L., Friedrich, M., Grootes, P. M., Guilderson, T. P., Hajdas, I., Heaton, T. J., Hogg, A. G., Hughen, K. A., Kromer, B., Manning, S. W., Muscheler, R., Palmer, J. G., Pearson, C., van der Plicht, J., Reimer, R. W., Richards, D. A., Scott, E. M., Southon, J. R., Turney, C. S. M., Wacker, L., Adolphi, F., Büntgen, U., Capano, M., Fahrni, S. M., Fogtmann-Schulz, A., Friedrich, R., Köhler, P., Kudsk, S., Miyake, F., Olsen, J., Reinig, F., Sakamoto, M., Sookdeo, A., and Talamo, S.: The IntCal20 Northern Hemisphere radiocarbon age calibration curve (0–55 cal. ka BP), *Radiocarbon*, 62, 725–757, <https://doi.org/10.1017/RDC.2020.41>, 2020.
- Reimer, P. J., Baillie, M. G., Bard, E., Beck, J. W., Buck, C. E., Blackwell, P. G., Burr, G. S., Cutler, K. B., Damon, P. E., Edwards, R. L., Fairbanks, R. G., Friedrich, M., Guilderson, T. P., Hogg, A. G., Hughen, K. A., Kromer, B., McCormac, G., Ramsey, C. B., Reimer, R. W., Remmele, S., Southon, J. R., Stuvier, M., Taylor, F. W., van der Plicht, J., and Weyhenmeyer, C. E.: IntCal04: A New Consensus Radiocarbon Calibration Dataset from 0–26 ka BP, *Radiocarbon*, 46, 1029–1058, 2004.
- Roth, R. and Joos, F.: A reconstruction of radiocarbon production and total solar irradiance from the Holocene  $^{14}\text{C}$  and  $\text{CO}_2$  records: implications of data and model uncertainties, *Clim. Past*, 9, 1879–1909, <https://doi.org/10.5194/cp-9-1879-2013>, 2013.
- Rubino, M., Etheridge, D. M., Thornton, D. P., Howden, R., Allison, C. E., Francey, R. J., Langenfelds, R. L., Steele, L. P., Trudinger, C. M., Spencer, D. A., Curran, M. A. J., van Ommen, T. D., and Smith, A. M.: Revised records of atmospheric trace gases  $\text{CO}_2$ ,  $\text{CH}_4$ ,  $\text{N}_2\text{O}$ , and  $\delta^{13}\text{C}\text{-CO}_2$  over the last 2000 years from Law Dome, Antarctica, *Earth Syst. Sci. Data*, 11, 473–492, <https://doi.org/10.5194/essd-11-473-2019>, 2019.
- Siegenthaler, U., Monnin, E., Kawamura, K., Spahni, R., Schwander, J., Stauffer, B., Stocker, T. F., Barnola, J.-M., and Fischer, H.: Supporting evidence from the EPICA Dronning Maud Land ice core for atmospheric  $\text{CO}_2$  changes during the past millennium, *Tellus B*, 57(7), 51–57, doi:10.1111/j.1600-0889.2005.00131.x, 2005.
- Vonmoos, M., Beer, J., and Muscheler, R.: Large variations in Holocene solar activity: Constraints from  $^{10}\text{Be}$  in the Greenland Ice Core Project ice core, *J. Geophys. Res.-Space*, 111, A10105, doi:10.1029/2005JA011500, 2006.